


Bremsstrahlung photons from a hadronizing quark-gluon plasmaTaesoo Song **GSI Helmholtzzentrum für Schwerionenforschung GmbH, Planckstrasse 1, 64291 Darmstadt, Germany*

(Received 15 October 2022; accepted 15 February 2023; published 27 February 2023)

Assuming that quark and antiquark numbers are separately conserved during hadronization, I calculate bremsstrahlung photons from a hadronizing quark-gluon plasma. The quark and antiquark numbers are obtained from the hadron numbers in the statistical model and the transition amplitudes for the hadronization from the constraint that all quarks and antiquarks must be consumed in the hadronization. Then bremsstrahlung photons from the hadronization are obtained in the soft photon approximation, and one finds that their contribution to the direct photons increases in low-energy heavy-ion collisions and in peripheral collisions where the lifetime of a quark-gluon plasma (QGP) is relatively short.

DOI: [10.1103/PhysRevC.107.024916](https://doi.org/10.1103/PhysRevC.107.024916)**I. INTRODUCTION**

Ultrarelativistic heavy-ion collisions produce an extremely hot and dense nuclear matter which is possibly related to the state of the early universe. Electromagnetic particles such as dileptons (virtual photons) and real photons are promising probe particles searching for the properties of the extreme matter. Since they have no strong charge, they do not interact with the produced matter but get through it without being interrupted. Therefore, they deliver the information of the matter at their production sites and times [1,2].

The produced photons in heavy-ion collisions are classified into decay photons and direct photons. The former is produced through the electromagnetic decay of hadrons, and the latter from the interactions of particles both in partonic and hadronic phases. The direct photons are more interesting, because they disclose the properties of the matter.

Several years ago it was measured at the BNL Relativistic Heavy Ion Collider (RHIC) and the CERN Large Hadron Collider (LHC) that the elliptic flows of direct photons in heavy-ion collisions are comparable to those of pions and decay photons, which is called the “direct photon puzzle,” because the direct photons are continually produced from the initial stage where elliptic flows are not developed yet [2–8]. One possible way to explain the large elliptic flows is that direct photons are mainly produced in the late stage, such as the hadronic phase [9], rather than in the partonic phase, and the out-of-equilibrium photon production might help it [10].

Production channels of direct photons in heavy-ion collisions are categorized according to production stage. The first one is the production before thermalization of the matter, which includes the primordial production and the preequilibrium one. The former is the production through the scattering of partons in the colliding nucleons, which is calculable in perturbative QCD. Since the same photon is produced in $p + p$

collisions, it can be scaled by the number of binary collisions in heavy-ion collisions. The latter is presently unclear and depends on the model for the preequilibrium matter [11–14].

The second and third ones are, respectively, partonic and hadronic productions after the thermalization. The dominant channels in QGP are $q(\bar{q}) + g \rightarrow q + \gamma$ and $q + \bar{q} \rightarrow g + \gamma$, while in the hadron gas phase $\pi + \pi \rightarrow \rho + \gamma$ and $\pi + \rho \rightarrow \pi + \gamma$, with π and ρ being changeable to K and K^* , respectively.

Another source of direct photons in both partonic and hadronic matter is bremsstrahlung photons, which are induced by the interactions of charged particles. In QGP, for example, $q(\bar{q}) + q(\bar{q})$ and $q(\bar{q}) + g$ scatterings can produce bremsstrahlung photons, because (anti)quarks have nonzero electric charge.

Hadronization is a kind of interaction which confines free (anti)quarks into a bound state of a hadron. However, photon production from hadronization has barely been studied [15–19]. According to the lattice calculations the phase transition is a crossover at small baryon chemical potential [20], and the hadronization will be a smooth continuous transition from the thermal distribution of free (anti)quarks to the thermal distribution of free hadrons [21]. Though it is not an instant interaction, the momentum changes of (anti)quarks through the hadronization will bring about the emission of bremsstrahlung photons. Since low-energy bremsstrahlung photons are not affected by microscopic process but by macroscopic process, the incoming and outgoing momenta of (anti)quarks are the only necessary input to study the production of low-energy bremsstrahlung photons [22,23].

Hadronization happens in an extremely nonperturbative region of QCD, and many aspects of it are not well known. In this study I rely on the statistical model to obtain quark and antiquark number densities at T_c , assuming that quark and antiquark numbers are separately conserved during the hadronization and they play the role of constituent quarks and constituent antiquarks of hadrons. The transition amplitudes for hadronization are determined from the constraint

*t.song@gsi.de

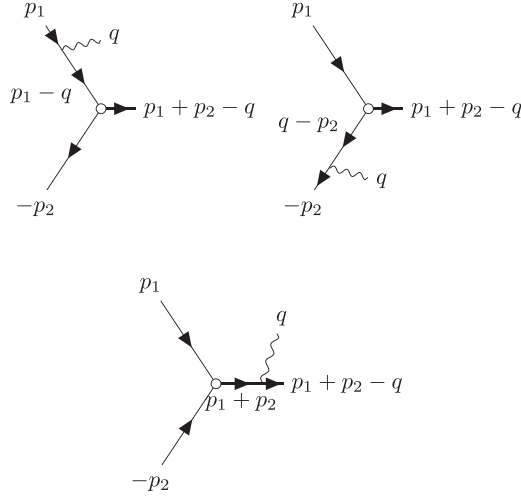


FIG. 1. Bremsstrahlung photon from quark and antiquark fusion to a meson, ignoring possible emission and/or absorption of soft gluons

that all quarks and antiquarks are consumed during the hadronization.

I first calculate the photon production from meson and baryon formations in Sec. II, which is applied to QGP in Sec. III to obtain the spectrum of bremsstrahlung photons per unit volume of hadronizing QGP. After comparing the results with experimental data, I give a summary in Sec. IV.

II. BREMSSTRAHLUNG PHOTONS FROM MESON/BARYON FORMATION

The momentum distribution of a radiated photon from decelerated charged particle i is expressed as [24–26]

$$\omega \frac{dN^\gamma}{d^3\mathbf{q}} = \frac{1}{2(2\pi)^3} \sum_\lambda |j_i \cdot \varepsilon^\lambda(q)|^2, \quad (1)$$

where $q_\mu = (\omega, \mathbf{q})$ is the photon energy and momentum, $(j_i)_\mu$ the electromagnetic current induced by the charged particle i , and $\varepsilon_\mu^\lambda(q)$ the polarization vector of the emitted photon with λ being the polarization state.

In Fig. 1 the transition amplitude for a quark and antiquark to form a meson with a photon emission is proportional to [24–26]

$$J \cdot \varepsilon^\lambda = \left\{ -Q_1 \frac{p_1^\mu}{p_1 \cdot q} - Q_2 \frac{p_2^\mu}{p_2 \cdot q} + Q_m \frac{(p_1 + p_2 - q)^\mu}{(p_1 + p_2 - q) \cdot q} \right\} \varepsilon_\mu^\lambda(q), \quad (2)$$

where Q_1 and Q_2 are, respectively, the electric charges of the quark and antiquark and $Q_m = Q_1 + Q_2$.

As for the three quarks which form a baryon,

$$J \cdot \varepsilon^\lambda = \left\{ -Q_1 \frac{p_1^\mu}{p_1 \cdot q} - Q_2 \frac{p_2^\mu}{p_2 \cdot q} - Q_3 \frac{p_3^\mu}{p_3 \cdot q} + Q_b \frac{(p_1 + p_2 + p_3 - q)^\mu}{(p_1 + p_2 + p_3 - q) \cdot q} \right\} \varepsilon_\mu^\lambda(q), \quad (3)$$

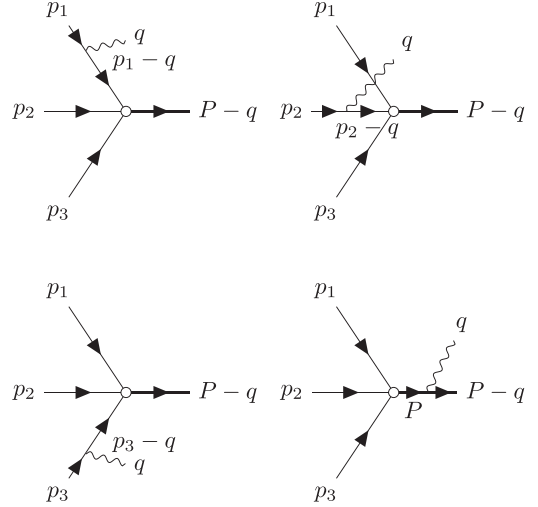


FIG. 2. Bremsstrahlung photon from three-quark fusion to a baryon, where $P = p_1 + p_2 + p_3$, ignoring possible emission and/or absorption of soft gluons

as shown in Fig. 2, with Q_1, Q_2 , and Q_3 being electric charges of the three quarks and $Q_b = Q_1 + Q_2 + Q_3$.

Substituting Eqs. (2) and (3) into Eq. (1) and using $\sum_\lambda \varepsilon_\mu^{\lambda*}(q) \varepsilon_\nu^\lambda(q) = -g_{\mu\nu}$, the photon spectrum from meson formation is given by

$$\begin{aligned} \omega \frac{dN_m^\gamma}{d^3\mathbf{q}} = & \frac{1}{2(2\pi)^3} \left[-Q_1^2 \frac{m_1^2}{(p_1 \cdot q)^2} - Q_2^2 \frac{m_2^2}{(p_2 \cdot q)^2} \right. \\ & - Q_m^2 \frac{(P - q)^2}{[(P - q) \cdot q]^2} - 2Q_1 Q_2 \frac{p_1 \cdot p_2}{(p_1 \cdot q)(p_2 \cdot q)} \\ & \left. + \frac{2Q_m}{(P - q) \cdot q} \left\{ Q_1 \frac{p_1 \cdot (P - q)}{(p_1 \cdot q)} + Q_2 \frac{p_2 \cdot (P - q)}{(p_2 \cdot q)} \right\} \right], \quad (4) \end{aligned}$$

where $P = p_1 + p_2$, and that from baryon formation is

$$\begin{aligned} \omega \frac{dN_b^\gamma}{d^3\mathbf{q}} = & \frac{1}{2(2\pi)^3} \left[- \sum_{i,j=1,2,3} Q_i Q_j \frac{p_i p_j}{(p_i \cdot q)(p_j \cdot q)} \right. \\ & - Q_b^2 \frac{(P - q)^2}{[(P - q) \cdot q]^2} \\ & \left. + \frac{2Q_b}{(P - q) \cdot q} \sum_{i=1,2,3} Q_i \frac{p_i \cdot (P - q)}{(p_i \cdot q)} \right], \quad (5) \end{aligned}$$

where $P = p_1 + p_2 + p_3$.

The above calculations are called the soft photon approximation, because each term in the curly brackets of Eqs. (2) and (3) is a propagator approximated in the limit of a soft photon ($q \ll p_i$), and it is assumed that the photon emission does not affect the main scattering which causes charge deceleration [23]. For the approximation to be valid, photon energy should be much smaller than scattering energy.

Figures 1 and 2 are reminiscent of the coalescence model which is widely used to describe the hadronization of quarks and antiquarks [27]. One drawback of the model is that

total energy is not conserved, as in, for example, the pion formation from a quark and antiquark pair. More correct or realistic Feynman diagrams will be accompanied by soft gluon emission and/or absorption, which affects the hadronization of other partons [21]. For instance, if the invariant mass of combined partons is smaller than the hadron mass, the deficient energy is supplied by absorbing soft gluons, while soft gluons are emitted in the opposite case. The gluon emission or absorption is more favored than that of photons because of much larger strong coupling than the coupling in QED. Therefore, the hadronization in Figs. 1 and 2 is not simply $n \rightarrow 1$, but it involves soft gluon emission and/or absorption, and the scattering energy is different from hadron mass. In the present study a photon is then attached to the hadronization process following the soft photon approximation.

III. PHOTONS FROM A HADRONIZING QGP

For simplicity, I assume that the transition amplitudes for (anti)quarks to form a meson (A_m), baryon (A_b), and antibaryon ($A_{\bar{b}}$) at T_c are constants as follows:

$$A_m \sum_{i,j=u,d,s} \int \frac{d^3 p_1}{(2\pi)^3} \frac{d^3 p_2}{(2\pi)^3} f_i(p_1) f_j(p_2) = n_m, \quad (6)$$

$$A_b \sum_{i,j,k=u,d,s} \int \frac{d^3 p_1}{(2\pi)^3} \frac{d^3 p_2}{(2\pi)^3} \frac{d^3 p_3}{(2\pi)^3} f_i(p_1) f_j(p_2) f_k(p_3) = n_b, \quad (7)$$

$$A_{\bar{b}} \sum_{i,j,k=u,d,s} \int \frac{d^3 p_1}{(2\pi)^3} \frac{d^3 p_2}{(2\pi)^3} \frac{d^3 p_3}{(2\pi)^3} \bar{f}_i(p_1) \bar{f}_j(p_2) \bar{f}_k(p_3) = n_{\bar{b}}, \quad (8)$$

where $f_i(p)$ is the Fermi-Dirac distribution of the parton i , including spin-color degeneracy, and n_m , n_b , and $n_{\bar{b}}$ are respectively the number densities of mesons, baryons, and antibaryons at $T_c = 0.16$ GeV. In the statistical model $n_m = 0.35 \text{ fm}^{-3}$ and $n_b = n_{\bar{b}} = 0.032 \text{ fm}^{-3}$ for $\mu_B = 0$, and $n_m = 0.35 \text{ fm}^{-3}$, $n_b = 0.056 \text{ fm}^{-3}$, and $n_{\bar{b}} = 0.0046 \text{ fm}^{-3}$ for $\mu_B = 200$ MeV. The former μ_B corresponds to LHC and RHIC energies and the latter μ_B to CERN Super Proton Synchrotron (SPS) energy [28].

$f_i(p)$ depends on the effective mass of the (anti)quark at T_c , which can be obtained from the assumption that all (anti)quarks are consumed through hadronization, that is,

$$\sum_{i=u,d,s} \int \frac{d^3 p}{(2\pi)^3} f_i(p) = n_m + 3n_b, \quad (9)$$

$$\sum_{i=u,d,s} \int \frac{d^3 p}{(2\pi)^3} \bar{f}_i(p) = n_m + 3n_{\bar{b}}.$$

Assuming that strange quark mass is same as up/down quark mass for simplicity, the (anti)quark mass is about 340 MeV at $\mu_B = 0$, and from Eq. (8)

$$A_m = n_m / (N_f n_q)^2 = 2.27 \times 10^2 \text{ GeV}^{-3},$$

$$A_b = A_{\bar{b}} = n_b / (N_f n_q)^3 = 3.02 \times 10^3 \text{ GeV}^{-6} \quad (10)$$

with flavor number $N_f = 3$ and quark number density $n_q = \int d^3 p / (2\pi)^3 f_q(p)$.

For $\mu_B = 200$ MeV, (anti)quark mass is taken to be 310 MeV and

$$A_m = n_m / (N_f n_q) / (N_f n_{\bar{q}}) = 1.87 \times 10^2 \text{ GeV}^{-3},$$

$$A_b = n_b / (N_f n_q)^3 = 2.96 \times 10^3 \text{ GeV}^{-6},$$

$$A_{\bar{b}} = n_{\bar{b}} / (N_f n_{\bar{q}})^3 = 1.72 \times 10^3 \text{ GeV}^{-6}. \quad (11)$$

I note that in Eq. (11) the quark chemical potential is 54 MeV, which is not exactly one third μ_B .

Photon production from unit volume of hadronized QGP is then given by

$$\omega \frac{dN^\gamma}{V d^3 \mathbf{q}} = A_m \sum_{i,j=u,d,s} \int \frac{d^3 p_1}{(2\pi)^3} \frac{d^3 p_2}{(2\pi)^3}$$

$$\times f_i(p_1) f_j(p_2) \omega \frac{dN_m^\gamma}{d^3 \mathbf{q}}$$

$$+ A_b \sum_{i,j,k=u,d,s} \int \frac{d^3 p_1}{(2\pi)^3} \frac{d^3 p_2}{(2\pi)^3} \frac{d^3 p_3}{(2\pi)^3}$$

$$\times f_i(p_1) f_j(p_2) f_k(p_3) \omega \frac{dN_b^\gamma}{d^3 \mathbf{q}}$$

$$+ A_{\bar{b}} \sum_{i,j,k=u,d,s} \int \frac{d^3 p_1}{(2\pi)^3} \frac{d^3 p_2}{(2\pi)^3} \frac{d^3 p_3}{(2\pi)^3}$$

$$\times \bar{f}_i(p_1) \bar{f}_j(p_2) \bar{f}_k(p_3) \omega \frac{dN_{\bar{b}}^\gamma}{d^3 \mathbf{q}}. \quad (12)$$

The upper limit of photon energy from meson formation is given by

$$(p_1 + p_2 - q)^2 \geq m_\pi^2, \quad (13)$$

and from (anti)baryon formation by

$$(p_1 + p_2 + p_3 - q)^2 \geq m_N^2 \quad (14)$$

with m_π and m_N being respectively pion and nucleon masses.

The photon energy should be much smaller than the scattering energy for the soft photon approximation to be valid [9]. In thermal equilibrium the parton distribution function is peaked around temperature, and so is the scattering energy. However, it does not mean that all thermal partons have little momentum at T_c , because some of them still have large momentum, as shown in the spectrum of thermal photons from QGP or from hadron gas (HG), which does not terminate at low p_T but reaches high p_T [4].

Though the photon energy is always smaller than the scattering energy according to the energy conservation in Eqs. (13) and (14), the condition for the soft photon approximation ($\omega \ll \sqrt{s}$) is not well satisfied as photon energy increases. The scattering cross section is expanded in term of photon energy divided by the energy scale of the scattering; only the leading term is taken in this study. There are systematic studies on the second leading terms in the expansion [24,29], which require the derivative of transition amplitude with respect to external momentum. Since I assume constant transition amplitudes for hadronization in Eqs. (6), (7), and (8), it is not possible to calculate the second leading terms in the present form. If the photon energy is not much smaller than the energy scale, subleading corrections will not be negligible

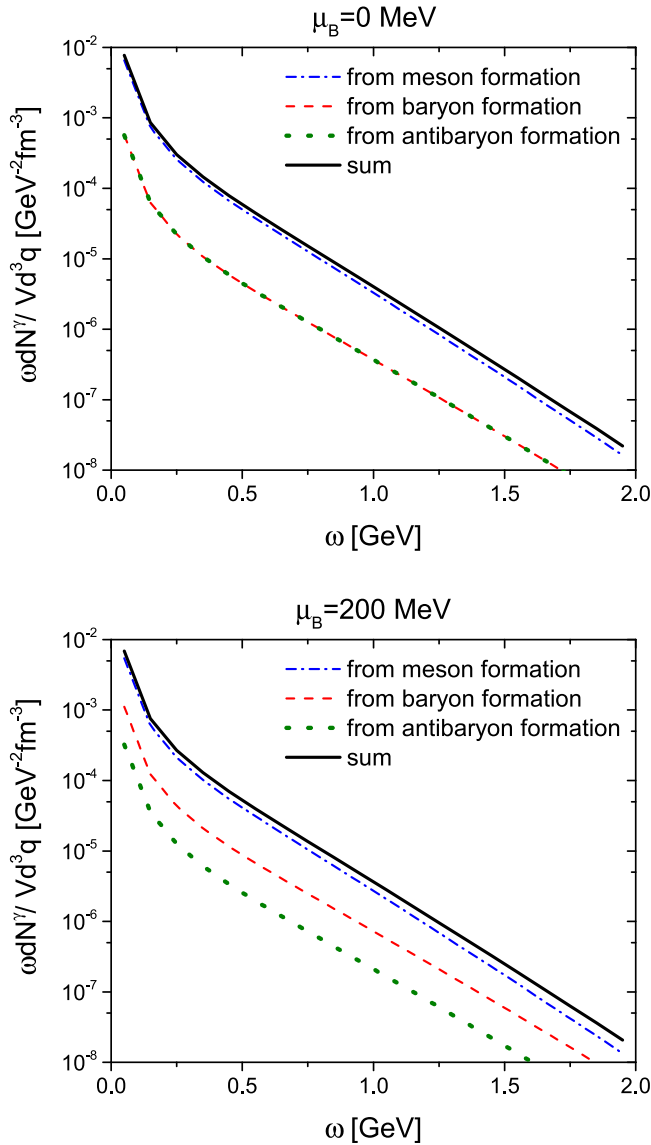


FIG. 3. Bremsstrahlung photon spectrum from unit volume (1 fm^3) of hadronizing QGP at $T_c = 160 \text{ MeV}$ for $\mu_B = 0$ (upper) and for $\mu_B = 200 \text{ MeV}$ (lower).

[9,24]. Since the underlying mechanism for hadronization is not well understood and/or not yet known, it is presently unclear whether the subleading terms will enhance or suppress the bremsstrahlung photons.

Figure 3 shows the spectra of bremsstrahlung photons from a unit volume (1 fm^3) of hadronizing QGP at $T_c = 160 \text{ MeV}$ for $\mu_B = 0$ and $\mu_B = 200 \text{ MeV}$. The contribution from meson formation is larger than that from (anti)baryon formation, since the meson density is much larger than that of (anti)baryons. On the other hand, the bremsstrahlung photons from (anti)baryon formation is a bit harder than that from meson formation. I note that the spectrum for $\mu_B = 0$ is about 10% larger at low momentum than that for $\mu_B = 200 \text{ MeV}$, partly due to the differences between Eqs. (10) and (11). It is interesting to see that the photon spectrum in Fig. 3 is

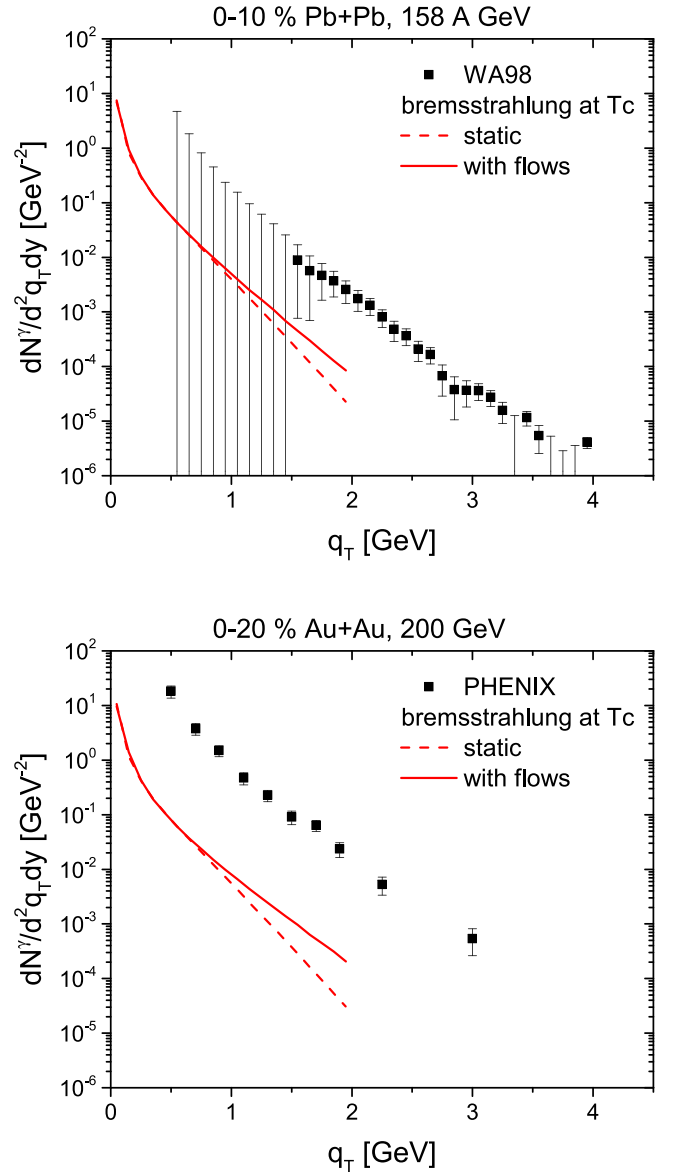


FIG. 4. Bremsstrahlung photon spectra as a function of transverse momentum in 0–10% central Pb + Pb collisions at $E_{\text{kin.}} = 158A \text{ GeV}$ and in 0–20% central Au + Au collisions at $\sqrt{s_{NN}} = 200 \text{ GeV}$ with and without considering transverse flows, compared with experimental data from the WA98 and PHENIX Collaborations [5,30].

comparable to the photon production rate in QGP as well as in HG near T_c , which is shown in Fig. 3 of Ref. [4]. I note that the coalescence photons are produced along a hypersurface at T_c while the production rate is thermal photons produced per unit time ($1 \text{ fm}c$) in matter.

One can compare the results with the experimental data in heavy-ion collisions, taking into account the volume of QGP at T_c , which can be deduced from charged particle or pion yield, assuming that the yield does not change after the chemical freeze-out temperature, which is almost same as T_c [28]. In the statistical model the number density of charged particles at $T = 160 \text{ MeV}$ is 0.367 fm^{-3} , and that of charged

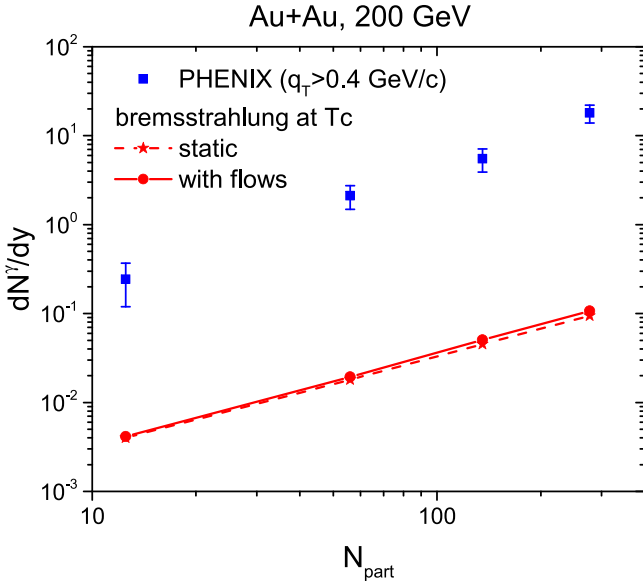


FIG. 5. Bremsstrahlung photon yield per rapidity for $q_T > 0.4$ GeV in Au + Au collisions at $\sqrt{s_{NN}} = 200$ GeV as a function of the number of participants, in comparison with the experimental data from the PHENIX Collaboration [5].

pions is 0.325 fm^{-3} including the feed-down from decays. The charged particle yield at midrapidity in 0–10% central Pb + Pb collisions at 158A GeV is roughly 400 [31], which can be interpreted as 1090 fm^3 of QGP volume at T_c . Similarly the charged pion yield in 0–20% central Au + Au collisions at $\sqrt{s_{NN}} = 200$ GeV, which is 448, is interpreted as 1380 fm^3 .

Figure 4 compares my results with the experimental data from the WA98 and PHENIX Collaborations [5,30]. The dashed lines are the spectra without considering transverse flows and the solid lines the spectra including the transverse flows, whose velocities are, respectively, 0.33 and 0.44 at T_c in the upper and lower panels from a schematic hydrodynamics [32]. Comparing the spectra in the upper and lower panels, one can see that the contribution from the bremsstrahlung photons at T_c is larger in central Pb + Pb collisions at $E_{\text{kin.}} = 158$ A GeV than in central Au + Au collisions at $\sqrt{s_{NN}} = 200$ GeV. The reason is that the direct photons are continually produced from or even before the formation of QGP to the freeze-out in heavy-ion collisions, while the bremsstrahlung photons from a hadronizing QGP are produced only once at T_c . Though the strong coupling α_s is large near T_c to force all partons to hadronize, abundant thermal photons overshadow the bremsstrahlung photons at T_c , if the lifetime of QGP is as long as in the central Au + Au collisions at $\sqrt{s_{NN}} = 200$ GeV. It means that the bremsstrahlung photons from a hadronizing QGP will be more visible in lower-energy heavy-ion collisions, and maximized when the collision energy of heavy ions barely reaches the phase boundary.

Figure 5 displays the bremsstrahlung photon yield per rapidity for $q_T > 0.4$ GeV in Au + Au collisions at $\sqrt{s_{NN}} = 200$ GeV as a function of the number of participants, compared with the experimental data from the PHENIX Collaboration [5]. Pion yields in 20–40%, 40–60%, and 60–92%

centralities from the PHENIX Collaboration [33] are, respectively, converted to 660, 264, and 58 fm^3 of QGP volume at T_c . The dashed line does not include flow effects and the solid line includes transverse flows at T_c , whose velocities are respectively 0.41, 0.33, and 0.21 in 20–40%, 40–60%, and 60–92% centralities from the schematic hydrodynamics [32]. Figure 5 shows that the contribution from the bremsstrahlung photon at T_c increases from central collisions to peripheral collisions. The reason is that the lifetime of nuclear matter is relatively short in peripheral collisions, which is consistent with Fig. 4.

IV. SUMMARY

Direct photons excluding decay photons and prompt photons are produced from a nuclear matter in heavy-ion collisions. There have been many studies on the photon production from QGP and from hadron gas, but the photon production from hadronization has barely been studied. In this work I have estimated, by using the soft photon approximation, the production of bremsstrahlung photons at hadronization where charged quarks and antiquarks change their momenta. For the calculations it is assumed that quark and antiquark numbers do not change during the hadronization and that a quark and an antiquark form a meson, three quarks form a baryon, and three antiquarks form an antibaryon. Since the statistical model provides the number density of each species of hadrons near T_c , one can deduce the number densities of quarks and antiquarks at T_c . For this, (anti)quark mass is taken to be 340 MeV for $\mu_B = 0$ and 310 MeV for $\mu_B = 200$ MeV, which are consistent with the constituent quark mass. The constant transition amplitudes for meson, baryon, and antibaryon formations are obtained from the constraint that all quarks and antiquarks must be consumed in hadronization.

I have found that the bremsstrahlung photons from meson formation are dominant over those from (anti)baryon formation, because more mesons are produced than (anti)baryons at T_c in the statistical model. But the spectrum from baryon formation is a bit harder than that of meson formation. I have also found that bremsstrahlung photon yield from hadronization is about 10% less at $\mu_B = 200$ MeV than at $\mu_B = 0$. It is interesting that the bremsstrahlung photons from a hadronizing QGP are comparable to the production rate of thermal photons per unit time (1 fm/c) in QGP or in HG near T_c .

With the number of charged particles or of charged pions interpreted as the volume of QGP, my calculations are compared with the experimental data on direct photon in heavy-ion collisions. I have found that the contribution from the bremsstrahlung photons at T_c to the direct photons produced in heavy-ion collisions increases in low-energy collisions and in peripheral collisions, because the thermal photons are continually produced from the initial stage of hot dense nuclear matter to the freeze-out, and their yield is proportional to the lifetime of the matter. Therefore, the contribution from the bremsstrahlung photons at T_c will be maximized, when the collision energy of heavy-ions barely reaches the phase boundary, and it may serve as a signal for the QGP formation in heavy-ion collisions.

ACKNOWLEDGMENTS

We acknowledge support by the Deutsche Forschungsgemeinschaft (DFG, German Research Foundation) through the grant CRC-TR 211 ‘Strong-interaction matter under extreme

conditions’ - Project No. 315477589 - TRR 211. The computational resources were provided by the LOEWE-Center for Scientific Computing and the ‘‘Green Cube’’ at GSI, Darmstadt.

-
- [1] O. Linnyk, E. L. Bratkovskaya, and W. Cassing, *Prog. Part. Nucl. Phys.* **87**, 50 (2016).
- [2] G. David, *Rep. Prog. Phys.* **83**, 046301 (2020).
- [3] C. Shen, U. W. Heinz, J.-F. Paquet, and C. Gale, *Phys. Rev. C* **89**, 044910 (2014).
- [4] J.-F. Paquet, C. Shen, G. S. Denicol, M. Luzum, B. Schenke, S. Jeon, and C. Gale, *Phys. Rev. C* **93**, 044906 (2016).
- [5] A. Adare *et al.* (PHENIX Collaboration), *Phys. Rev. C* **91**, 064904 (2015).
- [6] A. Adare *et al.* (PHENIX Collaboration), *Phys. Rev. C* **94**, 064901 (2016).
- [7] J. Adam *et al.* (ALICE Collaboration), *Phys. Lett. B* **754**, 235 (2016).
- [8] S. Acharya *et al.* (ALICE Collaboration), *Phys. Lett. B* **789**, 308 (2019).
- [9] H. C. Eggers, R. Tabti, C. Gale, and K. Haglin, *Phys. Rev. D* **53**, 4822 (1996).
- [10] A. Schäfer, O. Garcia-Montero, J.-F. Paquet, H. Elfner, and C. Gale, *Phys. Rev. C* **105**, 044910 (2022).
- [11] J. Berges, K. Reygers, N. Tanji, and R. Venugopalan, *Phys. Rev. C* **95**, 054904 (2017).
- [12] A. Monnai, *Int. J. Mod. Phys. A* **37**, 2230006 (2022).
- [13] A. Monnai, *J. Phys. G* **47**, 075105 (2020).
- [14] J. Churchill, L. Yan, S. Jeon, and C. Gale, *Phys. Rev. C* **103**, 024904 (2021).
- [15] H. van Hees, M. He, and R. Rapp, *Nucl. Phys. A* **933**, 256 (2015).
- [16] H. van Hees, C. Gale, and R. Rapp, *Phys. Rev. C* **84**, 054906 (2011).
- [17] R. Rapp, *PoS (CPOD 2013)*, 008 (2013).
- [18] O. Garcia-Montero, N. Löhner, A. Mazeliauskas, J. Berges, and K. Reygers, *Phys. Rev. C* **102**, 024915 (2020).
- [19] H. Fujii, K. Itakura, K. Miyachi, and C. Nonaka, *Phys. Rev. C* **106**, 034906 (2022).
- [20] S. Borsanyi, G. Endrodi, Z. Fodor, A. Jakovac, S. D. Katz, S. Krieg, C. Ratti, and K. K. Szabo, *J. High Energy Phys.* **11** (2010) 077.
- [21] T. Song and G. Coci, *Nucl. Phys. A* **1028**, 122539 (2022).
- [22] T. Song and P. Moreau, *Phys. Rev. D* **98**, 116007 (2018), 1810.08013.
- [23] T. Song, I. Grishmanovskii, and O. Soloveva, *Phys. Rev. D* **107**, 036009 (2023).
- [24] F. E. Low, *Phys. Rev.* **110**, 974 (1958).
- [25] V. Koch, B. Blättel, W. Cassing, and U. Mosel, *Phys. Lett. B* **236**, 135 (1990).
- [26] M. E. Peskin and D. V. Schroeder, *An Introduction to Quantum Field Theory* (Addison-Wesley, Reading, USA, 1995).
- [27] V. Greco, C. M. Ko, and P. Levai, *Phys. Rev. Lett.* **90**, 202302 (2003).
- [28] A. Andronic, P. Braun-Munzinger, K. Redlich, and J. Stachel, *arXiv:2101.05747*.
- [29] T. H. Burnett and N. M. Kroll, *Phys. Rev. Lett.* **20**, 86 (1968).
- [30] M. M. Aggarwal *et al.* (WA98 Collaboration), *arXiv:nucl-ex/0006007*.
- [31] M. C. Abreu *et al.* (NA50 Collaboration), *Phys. Lett. B* **530**, 43 (2002).
- [32] T. Song, K. C. Han, and C. M. Ko, *Phys. Rev. C* **83**, 024904 (2011).
- [33] S. S. Adler *et al.* (PHENIX Collaboration), *Phys. Rev. C* **69**, 034909 (2004).